

# Mobility Profile and Wheelchair Driving Skills of Powered Wheelchair Users: Sensor-Based Event Recognition Using a Support Vector Machine Classifier.

Athena K. Moghaddam, Joelle Pineau, Jordan Frank, Philippe Archambault, François Routhier, Thérèse Audet, Jan Polgar, François Michaud, and Patrick Boissy, Member IEEE.

**Abstract**— This paper presents a method to automatically recognize events and driving activities during the use of a powered wheelchair (PW). The method uses a support vector machine classifier, trained from sensor-based data from a datalogging platform installed on the PW. Data from a 3D accelerometer positioned on the back of the PW were collected in a laboratory space during PW driving tasks. 16-segmented events and driving activities (i.e. impacts from different side on different objects, rolling down or up on incline surface, going across threshold of different height) were performed repeatedly (n=25 trials) by one operator at three different speeds (slow, normal, high). We present results from an experiment aiming to classify five different events and driving activities from the sensor data acquired using the datalogging platform. Classification results show the ability of the proposed method to reliably segment 100% of events, and to identify the correct event type in 80% of events.

## I. INTRODUCTION

It is well recognized that mobility is an important factor for the social participation and quality of life of individuals. For people who live with locomotor impairments, mobility assistive devices such as manual wheelchairs, power wheelchairs, scooters, and other motorized vehicles can be facilitators of mobility [1]. In Canada, 5% of community living and 50% of 65 years and older individuals living in

institutions use manual or powered wheelchairs [2]. Using a PW is a complex task whose efficiency and safety are modulated by factors such as individual capacity, wheelchair driving skills, design and technology features of the PW, environmental considerations, driving the PW as an activity and interaction effects between these factors [3]. Although PW mobility has many potential benefits for users, PW incidents and accidents are not uncommon and their consequences can be serious [4-6]. While there is no extensive published evidence, such incidents are often caused by unsafe behavior, sometimes combined with poor wheelchair driving skills. To date, little research has explored PW mobility safety, and no gold standard exists to determine whether a user's skill-level makes him or her a safe driver in real life. To improve powered wheelchair driving skills of users and also wheelchair design in terms of safety and performance, a better characterization of wheelchair users' driving behavior is required, in various real and ecological indoor and outdoor settings [7].

A collaborative research program on PW use and its impact on mobility and social participation was started in 2008 with the purpose of developing and testing outcome measures and technology that can enhance effective and safe PW use in adults [8]. This paper presents a method to automatically recognize events and driving activities during use of a PW. The method trains a support vector machine classifier, using sensor-based data collected from a datalogging platform installed on a PW. The full dataset includes 16 segmented tasks and multiple sensor sources. Preliminary results focusing on automatically distinguishing between five of those events using data from one sensor source (3D accelerometer) are presented to test the robustness of the method.

## II. DATALOGGING PLATFORM FOR MONITORING PW USE

A proof of concept for a measurement approach to monitor real life use of PW was developed and is currently in use with a sample of PW users. The platform, called wireless inertial measurement units with GPS (WIMU-GPS) (Figure 1) consists of a datalogger with embedded sensors connected to external sensors installed on the PW. The sensors and components embedded into the WIMU-GPS consist of the following: inertial measurement unit (triaxial accelerometer, a triaxial gyroscope and a triaxial magnetometer, to compute pitch, yaw and roll angles of the module); a SIRFIII global

Manuscript received April 2, 2011. Corresponding author: P. Boissy. Work supported by the Natural Sciences and Engineering Research Council (NSERC) of Canada and the Canadian Institute of Health Research (CIHR).

A. K. Moghaddam, J. Pineau, J. Frank are with the School of Computer Science, McGill University, Montreal, QC CANADA. (akarde@cs.mcgill.ca, jordan.frank@cs.mcgill.ca, jpineau@cs.mcgill.ca).

P. S. Archambault is with the School of Physical and Occupational Therapy, McGill University, Montreal, QC, CANADA (philippe.archambault@mcgill.ca)

F. Routhier is with the Center for Interdisciplinary Research and Social Integration (CIRRS), Institut de réadaptation en déficience physique de Québec, Québec, QC CANADA (Francois.Routhier@rea.ulaval.ca).

T. Audet is with the Research Centre on Aging and with the Department of psychology, Faculty of Letters and Human Sciences, Université de Sherbrooke, Sherbrooke, QC CANADA (Therese.Audet@usherbrooke.ca)

J. Polgar is with School of Occupational Therapy, University of western Ontario, London, Ontario (jpolgar@uwo.ca).

F. Michaud is with the Dept of Electrical and Computer Engineering, Université de Sherbrooke (francois.michaud@usherbrooke.ca).

P. Boissy is with the Research Centre on Aging and with the Faculty of Medicine and Health Sciences, Université de Sherbrooke, Sherbrooke, QC, CANADA (Phone: 819-780-2220, ext.45628; fax 819-829-7141; e-mail: patrick.boissy@usherbrooke.ca).

positioning system (GPS) receiver; a 16-megahertz low power micro-processor and multiple I/O to connect external sensors; a Zigbee radio for wireless communication; a 2 Gb microSD card; a rechargeable 1 Ah Lithium-Ion battery. The external sensors include first a Force Sensing Resistor (FSR) array (3x3) mounted on a Plexiglas sheet fixed under the seat. Ultrasonic range finders (sonars) located at five positions on the PW (front, back, left, right and top) returns the distance to the nearest obstacles. The control signals from the user’s joystick are captured, allowing correlation of the user’s input with outcome (e.g., impact) for a specific environment. A wheel encoder counting the number of wheel revolutions provides the linear speed and an estimation of the distance traveled by the wheelchair. The platform is installed on the user’s PW by a technician and runs on its own battery. In this preliminary analysis, we used only the data from the 3D accelerometer. The rationale for this choice was to limit the number of sensor inputs in order to explore the power of the proposed event detection and classification methods under a set of distinct and similar driving tasks.

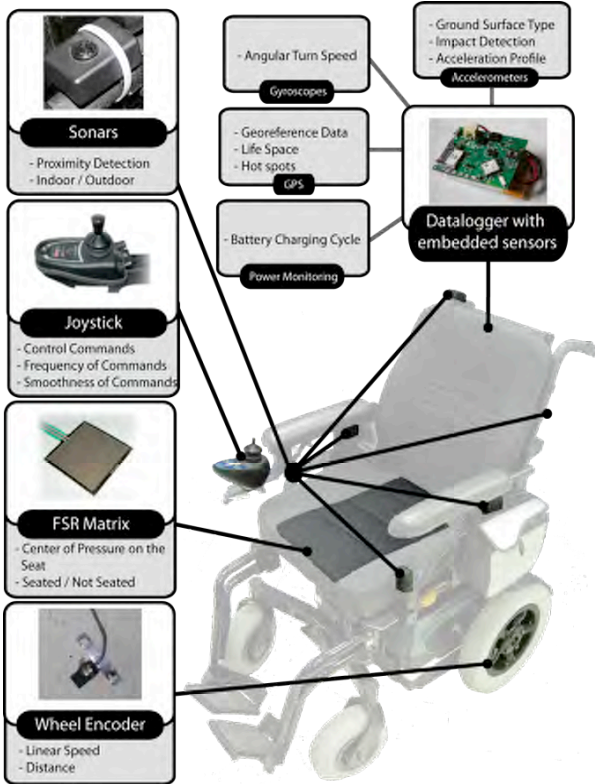


Figure 1. Overview of datalogging platform (WIMU-GPS)

### III. METHODS FOR ACTIVITY AND EVENT RECOGNITION USING SUPPORT VECTOR MACHINE CLASSIFIER

#### A. Data Acquisition Procedure

One user with no physical and cognitive impairments performed specific PW driving tasks under controlled conditions. 16 segmented tasks were performed repeatedly (n=25). Tasks varied (e.g., impacts from different sides on different objects, rolling up or down inclined surface, going across thresholds of different height) and were performed at

three different speeds (slow, normal, high). The execution of the tasks was standardized (i.e. start and completion of tasks were delimited, and distances when accomplishing the tasks were the same). Data from the 3D accelerometer of the WIMU-GPS positioned in the back of the PW seat were recorded for each repetition. Throughout the experiments reported below, we focused first on distinguishing between five different types of events (3 types of impacts and 2 driving activities.) These are listed in Table 1. The events and activities were selected to test the robustness of the classifier by choosing events with similar features.

TABLE 1. EVENT TYPES TO BE CLASSIFIED

| Label   | Event type                                      |
|---------|-------------------------------------------------|
| Class A | Rolling down 1 inch slope at slow speed         |
| Class B | Rolling down 1 inch slope at high speed         |
| Class C | Side impact to an object with normal speed      |
| Class D | Frontal impact to fixed object at normal speed  |
| Class E | Frontal impact to moving object at normal speed |

The dataset was divided into two sets: a training set and a validation set. For each event type, 15 recorded instances of the event were allocated to the training set, and 10 instances were allocated to the validation set.

#### B. Signal Processing

We calculated the magnitude of the acceleration (denoted  $x, y, z$ ) at each sample point, and normalized each parameter:

$$\beta = \sqrt{\left(\frac{x - \mu_x}{\sigma_x}\right)^2 + \left(\frac{y - \mu_y}{\sigma_y}\right)^2 + \left(\frac{z - \mu_z}{\sigma_z}\right)^2}$$

, where  $\mu$  is the mean of each parameter and  $\sigma$  is its variance along a window of size 28 sec, which is approximately the duration of one event. The signal  $\beta$  was then smoothed by performing a convolution with itself shifted by 0.4 sec.

#### C. Event Segmentation

The second phase consisted of extracting *events-of-interest* from the time series. At this point, the type of event was not considered; the goal was simply to identify segments of the data that feature notable events. Using the K-means algorithm [13], the full dataset (including all events, in both training and testing data) was divided into two classes: one was assumed to include the target events, whereas the other included the data points out of notable events window. Figure 2 presents a sample segmentation.

Labeled data were not available to formally evaluate the quality of the segmentation; quality was evaluated by visual inspection. This approach was reasonable for the current dataset, because the number and approximate timing of events were known. Using this simple method, we were able to correctly segment all known events. At this stage, we have identified events of interest but they are not classified by type of event.

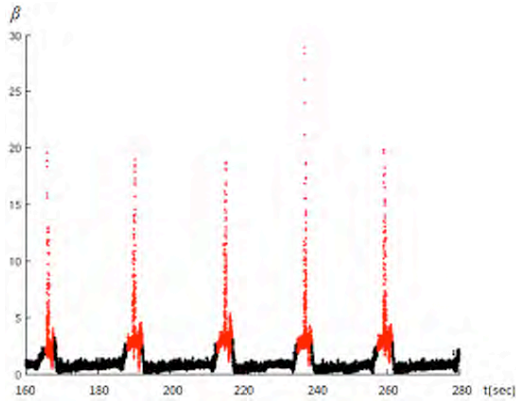


Figure 2. Input data is segmented into two groups: notable events (red) and general data (black)

#### D. Feature extraction

The method of time-delay embeddings was adopted for extracting the features necessary for the automatic labeling of events. The goal of time-delay embeddings is to capture the state and dynamics of an unknown dynamical systems from samples of that system [10]. This method has shown good properties in terms of automatically classifying dynamic events from accelerometer data [9].

Consider a time-series sampled at discrete intervals, where  $s_t$  is the sample taken at time  $t$ . We embed the signal in an  $m$ -

dimensional space:  $\tilde{s}_t^E = \left( s_t, s_{t-T}, s_{t-2T}, \dots, s_{t-(m-1)T} \right)$ , where  $m > 1$  and  $T > 1$  are parameters of the embedding process. Each point  $s_t^E \in \mathcal{R}^m$  in the embedding corresponds to an observation vector from the time-series. Principal components analysis is performed on the embedding of a set of points constructed as described above [11]. This produces a lower-dimensional embedding,  $s_t^E \in \mathcal{R}^k$  ( $k < m$ ), with reduced noise. This embedding is considered a sufficient model for the dynamic process that generated data, and can be used for various purposes, including generating new synthetic traces, or identifying distinct events, as in our case.

Using the data recorded as described above, we constructed separate embeddings for each event type, and accelerometer dimension. We denoted these  $X^i, Y^i, Z^i$ , where  $i \in \{A, B, C, D, E\}$  is the set of event types listed in Table 1. We used the same parameters,  $m=16$ ,  $T=0.1$ sec,  $k=5$ , to construct all embeddings. Note however that only datapoints extracted from event type  $i$  were used to build embeddings  $X^i, Y^i$  and  $Z^i$  (and similarly for each type of event).

Given a new segmented data point,  $(x_b, y_b, z_b)$ , we projected it into each embedding,  $X^i, Y^i, Z^i, \forall i$ . We then measured the distance between  $x_b^i$  and the closest point  $x$  in  $X^i$ :  $f(x_b^i) = \min_{x \in X^i} |x_b^i - x|^2$ , and similarly for  $Y^i$  and  $Z^i, \forall i$ . The set of measurements,  $f(x_b^i)$ , is the feature set used for the event classification step. Datapoints for each embedding are stored in a KD-tree, to permit fast nearest-neighbour lookup.

#### E. Event Classification

Given a dataset,  $D$ , where each point is described by a feature vector  $\{f(x_b^i), f(y_b^i), f(z_b^i)\}_{i=1..N}$ , supervised learning techniques can be applied to find a mapping from feature

space to event identity. For this step, we used a Support Vector Machine classifier [12], one of the most successful methods for classification tasks. The features extracted from the training set were used to build the embeddings, and to train the classifier. But whereas embeddings are built using data from a single event type, when training the classifier we considered features  $\{f(x_b^i), f(y_b^i), f(z_b^i)\}_{i=1..N}$ , thereby comparing the current point  $(x_b, y_b, z_b)$  to its nearest neighbour in embeddings of all event types. The superscript in the extraction vector denotes the projection of this point onto the embedding of event type  $i$  (and does not mean the point was collected while performing that event). The SVM was implemented with a degree=2 polynomial kernel. Rather than use multiclass classification, we considered a set of binary classifiers: each binary classifier decides whether the given feature vector is from class  $A$  or class  $B$  (and so on, for a total of 10 classifiers in the case of five event types); voting is used to obtain the final classification.

## IV. RESULTS

Using the approach outlined above, we report on the classification performance as measured on the testing dataset. Table 2 shows the confusion matrix, reporting, for each event type in the testing dataset, the number of samples that were classified as belonging to each of the five event types considered. We observe that a majority of samples from classes A, B and D were correctly classified, however a number of samples for classes C and E were misclassified.

TABLE 2. CONFUSION MATRIX SHOWING THE PROPORTION OF SAMPLES THAT ARE ATTRIBUTED TO EACH CLASS (REFER TO TABLE 1 FOR A GUIDE TO THE TYPES OF EVENTS.)

| True event type | Predicted class according to SVM classifier |               |               |               |        |
|-----------------|---------------------------------------------|---------------|---------------|---------------|--------|
|                 | A                                           | B             | C             | D             | E      |
| A               | <b>0.5599</b>                               | 0.1262        | 0.1150        | 0.0168        | 0.1821 |
| B               | 0.1530                                      | <b>0.7339</b> | 0.0667        | 0.0009        | 0.0456 |
| C               | 0.1593                                      | 0.2925        | <b>0.3751</b> | 0.0059        | 0.1671 |
| D               | 0.0010                                      | 0.0299        | 0.0008        | <b>0.9609</b> | 0.0074 |
| E               | <b>0.3578</b>                               | 0.1238        | 0.1875        | 0.0453        | 0.2855 |

Recall that the test set included five instances of each event type. Instead of considering the classification performance on a per-sample basis, we also considered the classification performance on a per-event basis. To automatically assign a classification for a full event, we assumed a majority voting rule, including all the samples from that event (considering only the events segmented as explained above). As shown in Table 3, overall, our approach correctly segmented and classified 80% of the events tested. All events from classes A, B and D were correctly classified. Events from class C were also mostly correctly classified, however four out of five events in the class E (*Frontal impact with moving object at normal speed*) were confused with class A (*Rolling down 1 inch slope in slow speed*).

**TABLE 3.** PREDICTION OF EACH EVENT IN THE TESTING SET ACCORDING TO THE SVM CLASSIFIER

| Instance | Class A | Class B | Class C | Class D | Class E |
|----------|---------|---------|---------|---------|---------|
| 1        | A       | B       | C       | D       | A       |
| 2        | A       | B       | C       | D       | A       |
| 3        | A       | B       | B       | D       | A       |
| 4        | A       | B       | C       | D       | E       |
| 5        | A       | B       | C       | D       | A       |

Figures 3, 4 and 5 show how some instances of activity type A, D and E are classified. In all three, purple represents activity A, B is blue, C is green, D is cyan, and E is red. The black points correspond to non-event samples. Similar figures for events from classes B and C are omitted due to lack of space. We observe that the time series containing events of type A and E share similar characteristics, however these figures show only the total (normalized) magnitude of the acceleration, not the features used for classification. We hypothesize that the use of additional sensor information would improve classification accuracy of class E events.

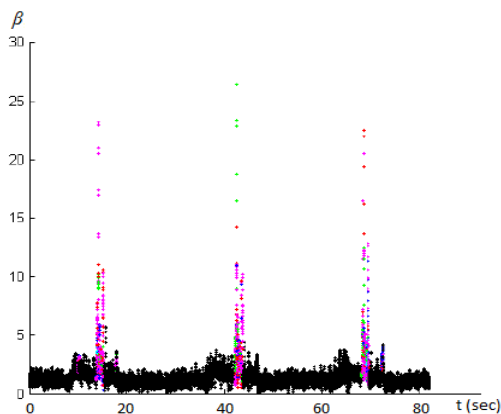


Figure 3. Classification of events of class A

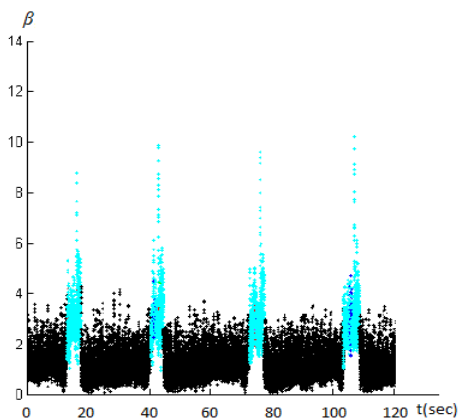


Figure 4. Classification of events of class D

## V. CONCLUSION

The proposed method reliably segmented PW events and driving activities and was able to identify the correct event type in 80% of events. Considering that only one source of

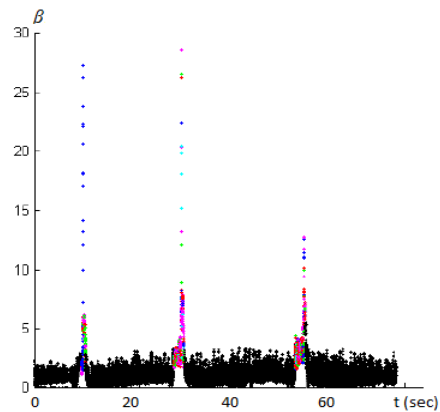


Figure 5. Classification of events of class E

sensor data (i.e. 3D accelerometer) was used and the event classification was performed on data with similar features, the results obtained support segmentation and classification method. In future experiments, we plan to expand the event identification methodology to draw a complete wheelchair users' behavior profile, and to link together measures related to global outcomes and driving performance (mean driving speed, distance traveled, etc.) with behavior in specifically identified events, such as collisions, maneuvering in tight corners, or driving on inclined surfaces. This research will be accomplished by characterizing PW use from multiple sensor sources in a controlled environment.

## REFERENCES

- [1] A. L. Salminen, *et al.*, "Mobility devices to promote activity and participation: a systematic review," *J Rehabil Med*, vol. 41, pp. 697-706, Sep 2009.
- [2] Shields M. Use of wheelchairs and other mobility support devices. Health Reports (Statistics Canada catalogue 82-003) 2004;15: 37-41.
- [3] A. Cook and J. Polgar, "A Framework for Assistive Technologies: the Human Activity Assistive Technology (HAAT) model," in *Assistive Technologies: Principles and Practice*: Mosby, 2007.
- [4] R. L. Kirby, *et al.*, "Wheelchair-related accidents caused by tips and falls among noninstitutionalized users of manually propelled wheelchairs in Nova Scotia," *Am J Phys Med Rehabil*, vol. 73, pp. 319-30, Sep-Oct 1994.
- [5] L. A. McClure, *et al.*, "Wheelchair repairs, breakdown, and adverse consequences for people with traumatic spinal cord injury," *Arch Phys Med Rehabil*, vol. 90, pp. 2034-8, Dec 2009.
- [6] S. Ummat and R. L. Kirby, "Nonfatal wheelchair-related accidents reported to the National Electronic Injury Surveillance System," *Am J Phys Med Rehabil*, vol. 73, pp. 163-7, Jun 1994.
- [7] H. Hoenig, *et al.*, "Methodological challenges confronting researchers of wheeled mobility aids and other assistive technologies," *Disabil Rehabil Assist Technol*, vol. 2, May 2007.
- [8] P. Boissy, M. Archambault, P., & Routhier, F., "Ecological measurement of powered wheelchair mobility and driving performance using event-driven identification and classification methods." in *Proceedings of RESNA*. 2008.
- [9] J. Frank, S. Mannor, D. Precup., "Activity and Gait Recognition with Time-Delay Embeddings," in *Proceedings of AAAI*, 2010.
- [10] H. Kantz, T. Schreiber, *Nonlinear time series analysis* Cambridge University Press, 2004.
- [11] I. Jolliffe, *Principal Component Analysis*. Springer. New York, 2002.
- [12] R. Collobert, S. Bengio, SVM-Torch: Support Vector Machines for Large-Scale Regression Problems, *Journal of Machine Learning Research*, vol 1, pages 143-160, 2001.
- [13] J. B. MacQueen (1967): "Some Methods for classification and Analysis of Multivariate Observations, Proceedings of 5-th Berkeley Symposium on Mathematical Statistics and Probability", 1:281-297.